

# All-dielectric Structure for Trapping Nanoparticles via Light Funneling and Nanofocusing

*Amir M. Jazayeri\* and Khashayar Mehrany*

Department of Electrical Engineering, Sharif University of Technology, Tehran 145888-9694, Iran

**KEYWORDS:** Optical Tweezers, all-dielectric structures, light funneling, nanofocusing, nanoantennas, electromagnetic force

**ABSTRACT:** We propose an all-dielectric structure which focuses the laser light well beyond the diffraction limit and thus considerably enhances the exerted optical trapping force upon dielectric nanoparticles. Although the structure supports a Fabry-Perot resonance, it actually acts as a nanoantenna in that the role of the Fabry-Perot resonance is to efficiently funnel the laser light into the structure. In other words, the nanoparticle to be trapped does not interact solely with the single resonant mode of the structure, but rather with a continuum of radiation modes in free space as well. Also, since the numerical results under the dipole approximation accord with the exact numerical results, ‘self-induced back-action trapping’ (SIBA), which has recently been coined in the context of optical resonators, is irrelevant to our proposed device. It is worth noting that no optical resonator supports SIBA when the nanoparticle size decreases to a few tens of nanometers. It should also be noted that SIBA actually provides neither a stronger trapping force nor a deeper trapping potential. These points together with some hitherto unappreciated subtleties will be discussed in this letter.

It is a well-known fact that microparticles can be trapped, controlled, and manipulated noninvasively via light<sup>1</sup>. Regrettably, however, the idea cannot be easily extended to include nanoparticles since the optical trapping force scales with the volume of the particle<sup>2</sup>. Optical tweezers are of much interest in that they give the means to scores of interesting applications in the physical and life sciences both<sup>3-9</sup>. The necessity of having optical trapping force stems from the inevitability of the particle's unwanted thermal motion. The trapping force is also referred to as the gradient force in that it pulls the particle toward a point where the electric field amplitude is locally maximum.

The gradient force becomes weak when the particle size shrinks. Since the negative permittivity of metals capacitates plasmonic resonance, one might be led to conclude that the exerted gradient force upon metal nanoparticles becomes large enough to facilitate optical trapping. However, it is only the real part of the polarizability of the particle which gives rise to the sought-after gradient force. The imaginary part of the polarizability leads to radiation pressure<sup>10</sup> pushing the object along the propagation direction and away from the trap. Also, the unwanted Ohmic loss in metal particles restricts the penetration depth of electromagnetic (EM) fields into the particle and therefore decreases the gradient force by making it proportional to the surface of the particle instead of its volume<sup>11,12</sup>. Besides, the Ohmic loss causes heat emission from the irradiated metal particle, which might damage either the particle or the surrounding medium<sup>13</sup>. Therefore, optical manipulation of metal particles is by no means easier than optical manipulation of dielectric particles.

One conceivable approach to alleviate the unwelcome trade-off between the particle size and the laser power required to ensure trapping is to focus light beyond the diffraction limit. In this fashion, the trapping force is enhanced neither by increasing the polarizability of the particle

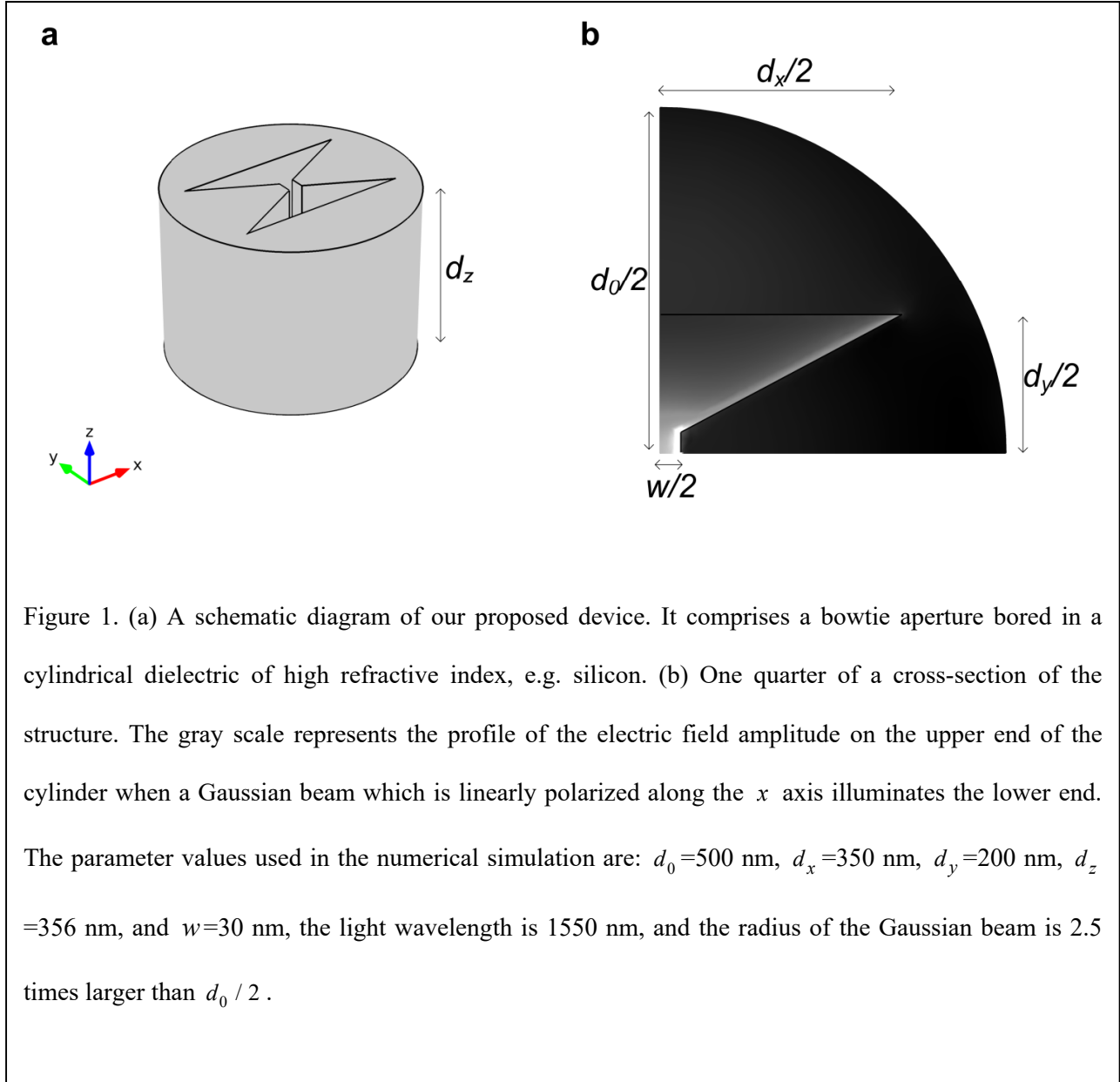
nor the laser power but rather by increasing the gradient of the electric field amplitude. This can be achieved by, for example, using the evanescent waves supported by total internal reflection at the interface between two dielectric media. However, while such evanescent waves can only accommodate trapping along the direction perpendicular to the interface, trapping within the tangential plane calls for further contrivance. It has been theoretically shown that two counter-propagating waves impinging upon planar glass-air interface can trap particles in the vicinity of a tungsten probe with diameter of about 20 nm<sup>14</sup>. The considerable amount of light scattering caused by the rather large refractive index of the tungsten probe plays an important role in shaping the electric field profile in such a manner that trapping is guaranteed within the tangential plane and along the normal direction both. More recently, plasmonic structures (e.g. gold microdisk<sup>15</sup>, gold nanodot<sup>16</sup>, and gold nanoblock pair<sup>17</sup>) have been employed to realize three-dimensional trapping of small particles by increasing the gradient of the electric field amplitude.

The use of optical resonators to trap particles was first proposed in 2006<sup>18,19</sup>. In particular, the term ‘self-induced trapping’, which was coined by Barth and Benson<sup>19</sup>, refers to the situation where the presence of the particle causes a *significant* shift (viz. a shift comparable with or larger than the linewidth of the resonator) in the resonance frequency of the resonator. In such a case, the laser frequency must be detuned from the bare resonance frequency (viz. from the resonance frequency in the absence of the particle). Self-induced trapping, which was subsequently called ‘self-induced back-action trapping’ (SIBA)<sup>20</sup>, has been experimentally demonstrated in photonic crystal cavities<sup>21</sup> as well as plasmonic cavities (e.g. rectangular aperture<sup>22</sup> and bowtie aperture<sup>23</sup> on gold film). A theoretical study of SIBA has recently been presented in ref 24.

Before we turn to our proposed device, we make some comments on SIBA. First, the term ‘SIBA’ is a misnomer in that back-action *always* exists when a particle and a resonator interact. More precisely, the resonance frequency is *always* sensitive to the position of the particle whenever the EM mode of the resonator contributes to the exerted gradient force upon the particle. Second, insofar as the magnitude of the gradient force and the depth of the trapping potential (viz. the line integral of the gradient force when the particle is moved from infinity to its current position) are concerned, SIBA offers *no* advantage, because SIBA enhances neither the electric field amplitude of the EM mode of the resonator nor its gradient. From this viewpoint, the whole purpose in detuning the laser frequency from the bare resonance frequency is to *compensate* for the significant resonance frequency shift induced by the presence of the particle, and thus to yield a large enough number of intracavity photons (or, equivalently, a strong enough electric field). However, the mean intracavity photon number, which is a function of the position of the particle, never exceeds the mean number of intracavity photons building up in the absence of the particle and detuning. Third, the real advantage offered by SIBA is the freedom it gives to change the trapping potential profile by changing the value of the detuning. For instance, one may increase the width of the trapping potential profile<sup>24</sup> *at the expense of* its depth. Fourth, since the lifetime of state-of-the-art optical resonators is hardly longer than a few nanoseconds, SIBA cannot take place when the particle size decreases to a few tens of nanometers. Fifth, one might mistakenly believe that a fictitious resonator with an infinitesimal linewidth is the ideal realization of SIBA. However, such a resonator responds to the particle’s motion so slowly that SIBA cannot take place. The theory presented in ref 24 about SIBA is based on the assumption that the resonator responds to the particle’s motion instantaneously. Sixth, the efficacy of a resonant structure in trapping nanoparticles is not necessarily a

manifestation of SIBA. Two examples of such a resonant structure are the structures proposed in refs 25 and 26.

In this letter, we propose an all-dielectric structure which is capable of trapping nanoparticles. The structure, which is schematically shown in Figure 1a, is a bowtie aperture bored in a cylindrical dielectric of high refractive index (e.g. silicon). We could also choose a non-circular cross-section for the dielectric (e.g. a square cross-section). Once the laser light which is linearly polarized along the  $x$  axis illuminates one end of the cylinder, a trapping force appears in the vicinity of the other end. The necessity of boring a bowtie aperture in a dielectric of high refractive index, finite thickness, and finite height can be understood by considering the following facts. First, EM fields can be confined within a slot (viz. a *non-square* rectangular aperture) bored in a dielectric of high refractive index. This one-dimensional confinement of EM fields within the slot (viz. the region of low refractive index) can be attributed to the continuity of the normal component of the electric displacement field<sup>6,27</sup>. Second, the desired two-dimensional confinement of EM fields, which is depicted in Figure 1b, is realized by reshaping the slot into a bowtie aperture so that the effective refractive index gradually increases as we move along the  $y$  axis toward the center of the bowtie aperture. This two-dimensional confinement of EM fields gives rise to the  $x$  and  $y$  components of the trapping force. Third, the  $z$  component of the trapping force comes from diffraction. Fourth, a Fabry-Perot resonance along the  $z$  axis, which is achieved by tuning  $d_z$ , ensures that the laser light is efficiently funneled into the structure. In the numerically calculated profile of the electric field amplitude plotted in Figure 1b, the radius of the Gaussian beam illuminating the structure is 2.5 times larger than the radius of the cylinder.



The nanoparticle to be trapped does *not* interact *solely* with the single resonant mode of the proposed Fabry-Perot resonator, but rather with a continuum of radiation modes in free space as well. This point can be understood by noting that the electric field around the trapping point is *not* a standing wave (or, equivalently, the time-averaged EM energy flux around the trapping point is not small). In fact, our proposed device acts as a nanoantenna which efficiently focuses the laser light well beyond the diffraction limit. It should also be noted that the numerical results presented later show that SIBA is irrelevant to our proposed device.

Since EM fields are time-harmonic, ‘time-averaged EM force’ is shortened to ‘EM force’ throughout this letter. The Maxwell stress tensor is employed to calculate the exerted EM force upon an object:

$$\vec{F} = \frac{1}{2} \text{Re} \left\{ \oint_S d\vec{S} \cdot \left[ \epsilon_0 \vec{E}^* \vec{E} + \frac{1}{\mu_0} \vec{B}^* \vec{B} - \frac{1}{2} \vec{I} (\epsilon_0 \vec{E}^* \cdot \vec{E} + \frac{1}{\mu_0} \vec{B}^* \cdot \vec{B}) \right] \right\} \quad (1)$$

where  $\vec{E}$  is the electric field phasor,  $\vec{B}$  is the magnetic field phasor,  $\vec{I}$  is the identity tensor,  $\epsilon_0$  and  $\mu_0$  are the permittivity and permeability of free space, respectively, and  $S$  is any closed surface which does not enclose any material body other than the object<sup>28</sup>. When the size of the object is much smaller than the light wavelength, the dipole approximation is usually invoked. Under the dipole approximation, the object is replaced with a linearly polarizable point-like dipole<sup>29</sup>. By applying the dipole approximation to eq 1, the  $z$  component of the EM force is simplified to:

$$F_{\text{dip}_z} = \frac{\alpha_R}{4} \partial(\vec{E}_i^* \cdot \vec{E}_i) / \partial z + \frac{\alpha_I}{2} \text{Im}[\vec{E}_i^* \cdot (\partial \vec{E}_i / \partial z)] \quad (2)$$

where  $\vec{E}_i$  is the *incident* electric field phasor (viz. the electric field phasor in the absence of the object), the object has been assumed to be non-magnetic,  $\alpha_R$  and  $\alpha_I$  are the real and imaginary parts of its polarizability, respectively, and the derivatives are calculated at the position of the object<sup>10</sup>. The EM force along other coordinate axes can be written in a similar fashion. The first term in eq 2 is the  $z$  component of the gradient force while the second term is the  $z$  component of radiation pressure. Assuming that the object is spherical and *low-loss*, its polarizability can be written as:

$$\alpha = 4\pi\epsilon_0 R^3 \alpha_0 / [1 + j2(k_0 R)^3 \alpha_0 / 3] \quad (3)$$

where  $k_0$  is the wavenumber in free space,  $R$  is the radius of the object, and  $\alpha_0$  denotes  $(\varepsilon - 1)/(\varepsilon + 2)$  in terms of its relative permittivity<sup>30</sup>. Although the imaginary part of the polarizability never vanishes, it becomes negligible when the object is loss-less (viz. when  $\text{Im}(\varepsilon)$  is zero). Since the nanoparticle we consider in the numerical examples is loss-less, we ignore radiation pressure whenever the results of eq 2 are presented.

Interestingly, the gradient force in eq 2 can also be derived by applying the dipole approximation to the method of virtual work instead of the Maxwell stress tensor. Under the dipole approximation, the presence of a small non-magnetic object does not significantly change the magnetic field. Therefore, the magnetic energy and the curl of the electric field are both almost insensitive to the position of the object. The insensitivity of the magnetic energy to the position of the object allows us to exclude it from the calculation of virtual work. The insensitivity of the curl of the electric field to the position of the object allows us to make use of the electrostatic result derived in ref 31. The electrostatic result states that the  $z$  component of the exerted electric force upon a linearly polarizable dipole  $\vec{\mathcal{P}}$  placed in an *initial* electrostatic field  $\vec{\mathcal{E}}_1$  whose sources are *fixed* is given by  $\frac{1}{2} \partial(\vec{\mathcal{P}} \cdot \vec{\mathcal{E}}_1) / \partial z$ . Since the electric field is time-harmonic in our problem, the  $z$  component of the time-averaged electric force in our problem is  $\frac{1}{4} \text{Re}[\partial(\vec{P}^* \cdot \vec{E}_1) / \partial z]$ , which equals  $\frac{\alpha_R}{4} \partial(\vec{E}_1^* \cdot \vec{E}_1) / \partial z$ , and corroborates the gradient force in eq 2.

Each of the EM modes excited by the laser contributes to  $\vec{E}_1$  in eq 2. If one of the EM modes belongs to a resonator, eq 2 states that the  $z$  component of the gradient force coming *solely* from that EM mode reads  $F_{\text{res,dip } z} = \frac{\alpha_R}{4} \partial(\vec{E}_{\text{res},i}^* \cdot \vec{E}_{\text{res},i}) / \partial z$ , where  $\vec{E}_{\text{res},i}$  is the electric

field phasor of the EM mode in the *absence* of the object. When SIBA takes place, the presence of the object causes a significant change in the mean number of intracavity photons, and therefore,  $F_{\text{res,dip}_z}$  is no longer equal to the  $z$  component of the actual gradient force coming from the EM mode. As a result, when SIBA takes place, eq 2 is no longer equal to the  $z$  component of eq 1. However, the numerical results presented below show that the results of eq 1 along the  $z$  axis (and along other coordinate axes) do not differ considerably from those of eq 2 (and its counterparts along other coordinate axes), and therefore, SIBA is irrelevant to our proposed device.

Before we present the numerical results, we discuss an hitherto unappreciated subtlety: whether or not SIBA takes place in a resonator,  $F_{\text{res,dip}_z}$  divided by the mean intracavity photon number in the *absence* of the object is equal to the  $z$  component of the actual gradient force coming from the EM mode of the resonator divided by the mean intracavity photon number in the *presence* of the object. This point can be understood by looking into the Hamiltonian describing the interaction *solely* between the object and the EM mode. The Hamiltonian reads  $\hbar\hat{N}[\omega_{\text{res}}(\hat{r}) - \omega_{\text{res}_0}]$ , where  $\hbar$  is the reduced Planck constant,  $\hat{N}$  is the intracavity photon number operator, and  $\omega_{\text{res}}(\hat{r}) - \omega_{\text{res}_0}$  is the change in the resonance frequency of the EM mode as a function of the center-of-mass position operator  $\hat{r}$  of the object. As a result, the  $z$  component of the gradient force operator coming from the EM mode is given by  $\hat{F}_{\text{res}_z} = -\hbar\hat{N}\partial\omega_{\text{res}}(\hat{r})/\partial\hat{z}$ . Since quantum fluctuations are irrelevant to our problem, the  $z$  component of the gradient force coming from the EM mode can be written as  $F_{\text{res}_z} = -\hbar\bar{N}\partial\omega_{\text{res}}/\partial z$ , where the mean intracavity photon number  $\bar{N}$  and the resonance frequency  $\omega_{\text{res}}$  are functions of the center-of-mass position

$\vec{r}$  of the object. Interestingly, if one calculates  $\partial\omega_{\text{res}} / \partial z$  by a perturbation method, it can be seen that  $F_{\text{res},z} / \bar{N}$  accords with  $F_{\text{res,dip},z} / \bar{N}_0$ , where  $\bar{N}_0$  denotes the mean intracavity photon number in the *absence* of the object.

We use the finite element method (COMSOL Multiphysics) to numerically calculate  $\vec{E}$  and  $\vec{B}$  in eq 1 as well as  $\vec{E}_i$  in eq 2. In all the numerical examples, we make the following assumptions about our proposed device, which is schematically shown in Figure 1: (i) the cylinder is made of silicon, and its refractive index is 3.45; (ii) the light wavelength in free space is 1550 nm, and thus, silicon is loss-less; (iii) the diameter of the cylinder (viz. the geometrical parameter  $d_0$ ) is 500 nm; (iv) the geometrical parameters  $d_x$  and  $d_y$  are 350 nm and 200 nm, respectively; (v) the lower end of the cylinder is placed at the focal plane of a conventional lens whose numerical aperture is 0.8, or, equivalently, the radius of the Gaussian beam illuminating the structure is 617 nm (viz. 2.5 times larger than the radius of the cylinder); (vi) the nanoparticle to be trapped is a loss-less dielectric sphere of refractive index 2 and diameter 10 nm; (vii) the laser power is 1 mW, and thus, the numerical results are normalized to 1 mW of the laser power; (viii) the origin of the coordinate system lies at the upper end of the cylinder.

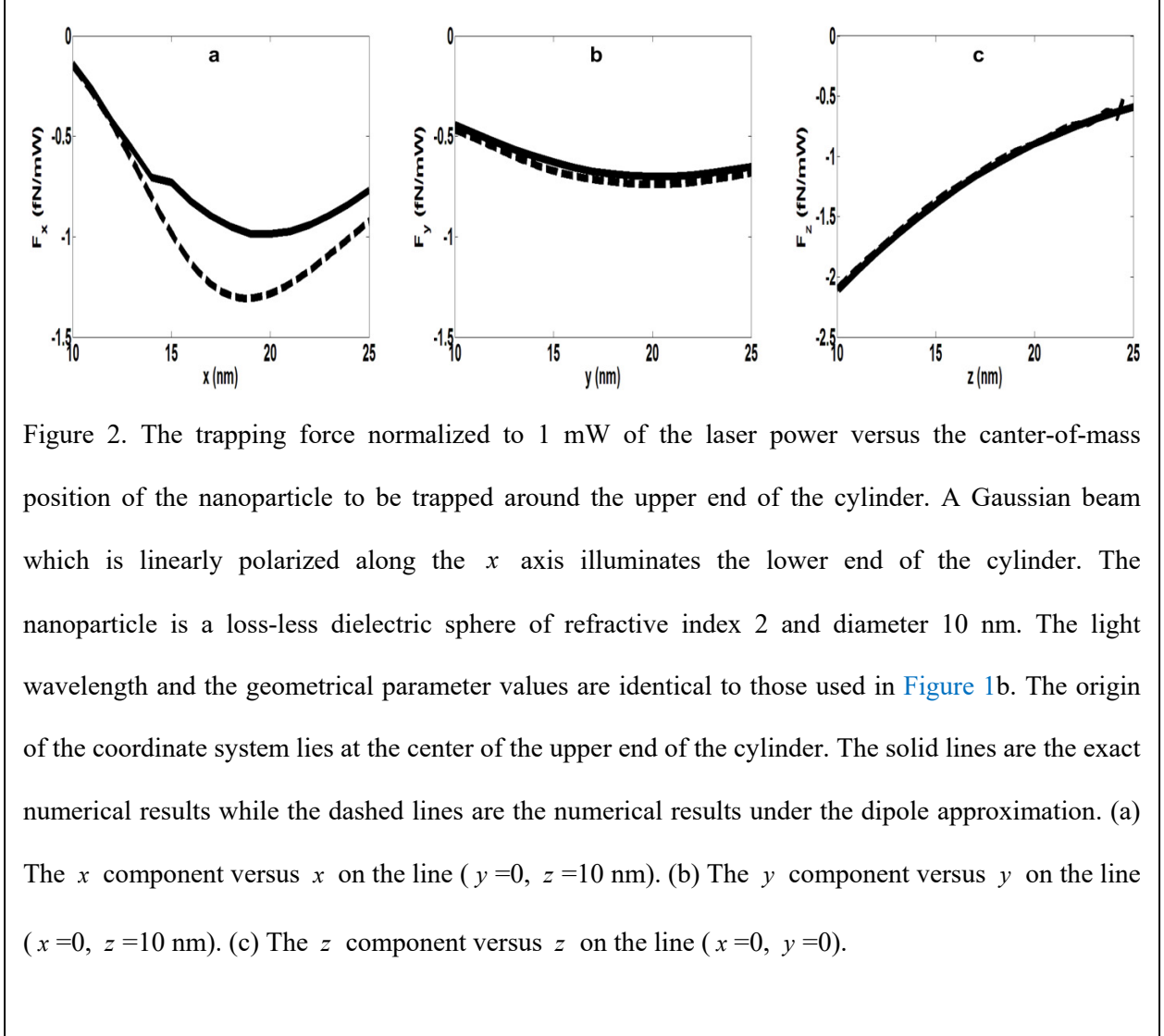


Figure 2. The trapping force normalized to 1 mW of the laser power versus the center-of-mass position of the nanoparticle to be trapped around the upper end of the cylinder. A Gaussian beam which is linearly polarized along the  $x$  axis illuminates the lower end of the cylinder. The nanoparticle is a loss-less dielectric sphere of refractive index 2 and diameter 10 nm. The light wavelength and the geometrical parameter values are identical to those used in Figure 1b. The origin of the coordinate system lies at the center of the upper end of the cylinder. The solid lines are the exact numerical results while the dashed lines are the numerical results under the dipole approximation. (a) The  $x$  component versus  $x$  on the line ( $y=0, z=10$  nm). (b) The  $y$  component versus  $y$  on the line ( $x=0, z=10$  nm). (c) The  $z$  component versus  $z$  on the line ( $x=0, y=0$ ).

In the first set of numerical examples, the geometrical parameter  $w$  is 30 nm. The height of the structure (viz. the geometrical parameter  $d_z$ ) is 356 nm. At this height, the optical power funneled into the structure is maximized on account of the Fabry-Perot resonance along the  $z$  axis. One might expect to achieve the maximum trapping force at this  $d_z$ , but the trapping force is maximized when  $d_z$  is 364 nm, in that the trapping force depends not only on the optical power funneled into the structure but also on the gradient of the field intensity. However, the trapping force is *not* very sensitive to  $d_z$ . Numerical calculations show that  $d_z$  can be changed in the range from 345 nm to 382 nm and the trapping force drops only by 10% from its optimum

value. Therefore, the performance of the structure is not very sensitive to  $d_z$ . The  $x$ ,  $y$ , and  $z$  components of the trapping force versus  $x$  on the line ( $y=0$ ,  $z=10$  nm), versus  $y$  on the line ( $x=0$ ,  $z=10$  nm), and versus  $z$  on the line ( $x=0$ ,  $y=0$ ) are plotted in [Figure 2a-c](#), respectively. In these figures, the solid lines are obtained by calculating [eq 1](#) while the dashed lines are obtained by calculating the gradient force in [eq 2](#) (and its counterparts along other coordinate axes). The maximum values of the  $x$  and  $y$  components of the trapping force on the lines ( $y=0$ ,  $z=10$  nm) and ( $x=0$ ,  $z=10$  nm) are 1.0 fN and 0.7 fN, respectively. The  $z$  component of the trapping force at ( $x=0$ ,  $y=0$ ,  $z=10$  nm) is 2.1 fN. The maximum value of the  $z$  component of the trapping force on the line ( $x=0$ ,  $y=0$ ) is 3.0 fN.

The trapping force can be increased by decreasing  $w$ . In the second set of numerical examples,  $w$  is reduced to 15 nm. The  $x$ ,  $y$ , and  $z$  components of the trapping force versus  $x$  on the line ( $y=0$ ,  $z=10$  nm), versus  $y$  on the line ( $x=0$ ,  $z=10$  nm), and versus  $z$  on the line ( $x=0$ ,  $y=0$ ) are plotted in [Figure 3a-c](#), respectively. The maximum values of the  $x$  and  $y$  components of the trapping force on the lines ( $y=0$ ,  $z=10$  nm) and ( $x=0$ ,  $z=10$  nm) are both 1.2 fN. The  $z$  component of the trapping force at ( $x=0$ ,  $y=0$ ,  $z=10$  nm) is now 4.4 fN. More importantly, the maximum value of the  $z$  component of the trapping force on the line ( $x=0$ ,  $y=0$ ) is now about 15 fN (viz. 5 times larger than the corresponding value when  $w$  is 30 nm). For a given value of  $w$ , one could further increase the trapping force by *simultaneously* optimizing the values of  $d_0$ ,  $d_x$ ,  $d_y$ , and  $d_z$ . However, the geometrical parameter values used in the numerical examples presented above are not optimized.

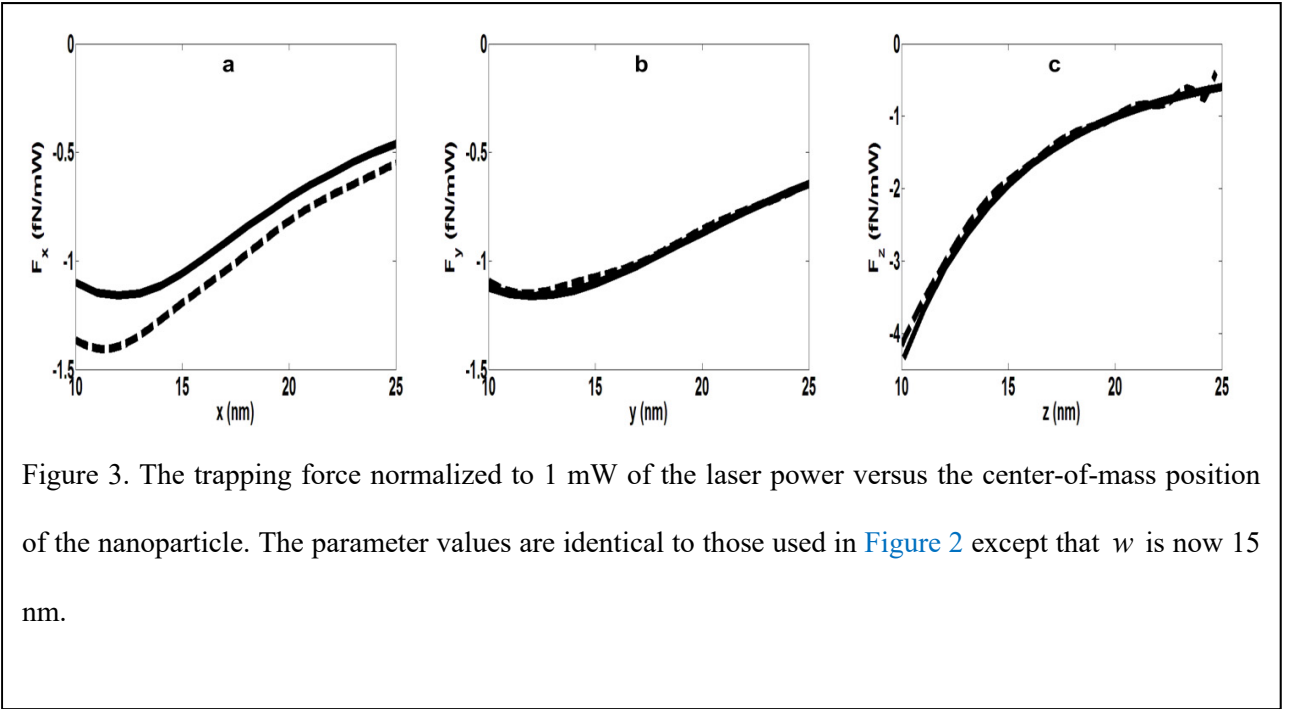


Figure 3. The trapping force normalized to 1 mW of the laser power versus the center-of-mass position of the nanoparticle. The parameter values are identical to those used in Figure 2 except that  $w$  is now 15 nm.

It is emphasized that the light wavelength in free space is 1550 nm in the numerical examples presented above, whereas the optical tweezers proposed in the recent literature usually enjoy smaller light wavelengths. For instance, the light wavelength in free space is 692 nm in ref 26. Also, the numerical results presented above are normalized to 1 mW of the laser power, whereas the results reported in the literature are not necessarily normalized to the laser power. For instance, the numerical results in ref 26 are normalized to the *transmitted* optical power, which is smaller than the laser power.

To investigate how much enhancement in the trapping force is achieved with our proposed device, we compare the numerical results presented above against the gradient force in the absence of the structure. Since the electric field profile of the laser light passing through the lens is Gaussian<sup>32</sup>, and the size of the nanoparticle is much smaller than the light wavelength, the gradient force in the absence of our proposed device can be calculated analytically by using eq 2. It can be seen that the maximum value of the  $z$  component of the calculated gradient force

normalized to the laser power is equal to  $0.3NA^4(k_0R)^3\alpha_0/c$ , where  $c$  is the speed of light in free space,  $NA$  is the numerical aperture of the lens, and  $k_0$ ,  $R$ , and  $\alpha_0$  retain their previous definitions in eq 3. Therefore, assuming the same parameter values used in the numerical examples presented above, there is a 2000-fold enhancement in the  $z$  component of the trapping force when the structure with  $w=30$  nm is employed. Only 1% of the 2000-fold enhancement in the trapping force comes from a 20-fold enhancement in the field intensity, while the remaining 99% comes from an enhancement in the gradient of the field intensity normalized to the field intensity. Finally, there is a 10000-fold enhancement in the trapping force when the structure with  $w=15$  nm is employed. Only 0.5% of the 10000-fold enhancement in the trapping force comes from a 50-fold enhancement in the field intensity, while the remaining 99.5% comes from an enhancement in the gradient of the field intensity normalized to the field intensity.

## AUTHOR INFORMATION

### Corresponding Author

\*Email: [jazayeri@ee.sharif.edu](mailto:jazayeri@ee.sharif.edu).

## ACKNOWLEDGEMENTS

A. M. Jazayeri is indebted to Farhad A. Namin for providing the computer equipment used to carry out the numerical simulations.

## REFERENCES

- (1) Ashkin, A. *Phys. Rev. Lett.* **1970**, 24, 156-159.
- (2) Maragò, O. M.; Jones, P. H.; Gucciardi, P. G.; Volpe, G.; Ferrari, A. C. *Nat. Nanotechnol.* **2013**, 8, 807-819.

- (3) Kiesel, N.; Blaser, F.; Delić, U.; Grass, D.; Kaltenbaek, R.; Aspelmeyer, M. *Proc. Nat. Acad. Sci.* **2013**, 110, 14180-14185.
- (4) Li, T.; Kheifets, S.; Raizen M. G. *Nat. Phys.* **2011**, 7, 527-530.
- (5) Gieseler, J.; Deutsch, B.; Quidant, R.; Novotny, L. *Phys. Rev. Lett.* **2012**, 109, 103603.
- (6) Yang, A. H.; Moore, S. D.; Schmidt, B. S.; Klug, M.; Lipson, M.; Erickson, D. *Nature* **2009**, 457, 71-75.
- (7) Pang, Y.; Song, H.; Kim, J. H.; Hou, X.; Cheng, W. *Nat. Nanotechnol.* **2014**, 9, 624-630.
- (8) Al Balushi, A. A.; Gordon, R. *Nano Lett.* **2014**, 14, 5787-5791.
- (9) Chen, Y. F.; Serey, X.; Sarkar, R.; Chen, P.; Erickson, D. *Nano Lett.* **2012**, 12, 1633-1637.
- (10) Chaumet, P. C.; Rahmani, A. *Opt. Exp.* **2009**, 17, 2224-2234.
- (11) Svoboda, K.; Block, S. M. *Opt. Lett.* **1994**, 19, 930-932.
- (12) Hansen, P. M.; Bhatia, V. K.; Harrit, N.; Oddershede, L. *Nano Lett.* **2005**, 5, 1937-1942.
- (13) Seol, Y.; Carpenter, A. E.; Perkins, T. T. *Opt. Lett.* **2006**, 31, 2429-2431.
- (14) Chaumet, P.C.; Rahmani, A.; Nieto-Vesperinas, M. *Phys. Rev. Lett.* **2002**, 88, 123601.
- (15) Righini, M.; Volpe, G.; Girard, C.; Petrov, D.; Quidant, R. *Phys. Rev. Lett.* **2008**, 100, 186804.
- (16) Grigorenko, A. N.; Roberts, N. W.; Dickinson, M. R.; Zhang, Y. *Nat. Photonics* **2008**, 2, 365-370.
- (17) Tanaka, Y.; Kaneda, S.; Sasaki, K. *Nano Lett.* **2013**, 13, 2146-2150.
- (18) Rahmani, A.; Chaumet, P. C. *Opt. Exp.* **2006**, 14, 6353-6358.
- (19) Barth, M.; Benson, O. *Appl. Phys. Lett.* **2006**, 89, 253114.
- (20) Juan, M. L.; Gordon, R.; Pang, Y.; Eftekhari, F.; Quidant, R. *Nat. Phys.* **2009**, 5, 915-919.
- (21) Descharmes, N.; Dharanipathy, U. P.; Diao, Z.; Tonin, M.; Houdré, R. *Phys. Rev. Lett.* **2013**, 110, 123601.
- (22) Chen, C.; Juan, M. L.; Li, Y.; Maes, G.; Borghs, G.; Van Dorpe, P.; Quidant, R. *Nano Lett.* **2011**, 12, 125-132.
- (23) Berthelot, J.; Acimović, S. S.; Juan, M. L.; Kreuzer, M. P.; Renger, J.; Quidant, R. *Nat. Nanotechnol.* **2014**, 9, 295-299.

- (24) Neumeier, L.; Quidant, R.; Chang, D. E. *New J. Phys.* **2015**, 17, 123008.
- (25) Righini, M.; Ghenuche, P.; Cherukulappurath, S.; Myroshnychenko, V.; García de Abajo, F. J.; Quidant R. *Nano Lett.* **2009**, 9, 3387-3391.
- (26) Saleh, A. A.; Dionne, J. A. *Nano Lett.* **2012**, 12, 5581-5586.
- (27) Almeida, V. R.; Xu, Q.; Barrios, C. A.; Lipson, M. *Opt. Lett.* **2004**, 29, 1209-1211.
- (28) Jazayeri, A. M.; Mehrany, K. *Phys. Rev. A* **2014**, 89, 043845.
- (29) Bohren, C. F.; Huffman, D. R. *Absorption and scattering of light by small particles*; John Wiley & Sons: New York, 1983.
- (30) Draine, B. T. *Astrophys. J.* **1988**, 333, 848-872.
- (31) Jackson, J. D. *Classical Electrodynamics*; John Wiley & Sons: Hoboken, 1999.
- (32) Saleh, B. E. A.; Teich, M. C. *Fundamentals of photonics*; John Wiley & Sons: New York, 1991.